PERGAMON

International Journal of Solids and Structures 39 (2002) 2109–2128

INTERNATIONAL JOURNAL OF SOLIDS and STRUCTURES

www.elsevier.com/locate/ijsolstr

3-D second-order plastic-hinge analysis accounting for lateral torsional buckling

Seung-Eock Kim [a,*], Jaehong Lee [b], Joo-Soo Park [a]

[a] *Department of Civil and Environmental Engineering/Construction Tech., Research Institute, Sejong University, 98 Koonja-dong Kwangjin-ku, Seoul 143-747, South Korea*

[b] *Department of Architectural Engineering/Construction Tech., Sejong University, 98 Koonja-dong Kwangjin-ku, Seoul 143-747, South Korea*

Received 24 July 2001; received in revised form 26 December 2001

Abstract

In this paper, 3-D second-order plastic-hinge analysis accounting for lateral torsional buckling is developed. This analysis accounts for material and geometric nonlinearities of the structural system and its component members. Moreover, the problem associated with conventional second-order plastic-hinge analyses, which do not consider the degradation of the flexural strength caused by lateral torsional buckling, is overcome. Efficient ways of assessing steel frame behavior including gradual yielding associated with residual stresses and flexure, second-order effect, and geometric imperfections are presented. In this study, a model consisting of the unbraced length and cross-section shape is used to account for lateral torsional buckling. The proposed analysis is verified by the comparison of the other analyses and load and resistance factor design results. A case study shows that lateral torsional buckling is a very crucial element to be considered in second-order plastic-hinge analysis. The proposed analysis is shown to be an efficient, reliable tool ready to be implemented into design practice.

Keywords: Plastic-hinge; Second-order analysis; Lateral torsional buckling; Steel frame; Load and resistance factor design

1. Introduction

In the current engineering practice, the interaction between the structural system and its component members is represented by the effective length factor. The effective length method generally provides a good design of framed structures. However, despite its popular use in the past and present as a basis for design, the approach has its major limitations. The first of these is that it does not give an accurate indication of the factor against failure, because it does not consider the interaction of strength and stability between the member and structural system in a direct manner. It is well-recognized fact that the actual failure mode of the structural system often does not have any resemblance whatsoever to the elastic buckling mode of the structural system that is the basis for the determination of the effective length factor K. The second and

* Corresponding author. Tel.: +82-2-3408-3391; fax: +82-2-3408-3332.
E-mail address: sekim@sejong.ac.kr (S.-E. Kim).

0020-7683/02/$ - see front matter
PII: S0020-7683(02)00082-3

Nomenclature

A, L area and length of beam-column element
C_b equivalent moment factor
C_w warping constant
E modulus of elasticity
E_t CRC (column research council) tangent modulus
F_r compressive residual stress
F_{yw} yield stress of web
F_{yf} yield stress of flange
G shear modulus of elasticity of steel
I_y, I_z moment of inertia with respect to y- and z-axes
J torsional constant
k_c, k_s coefficients accounting for situation where a large number of columns in a story and stories in a frame would reduce the total magnitude of geometric imperfections
k_{iiy}, k_{ijy}, k_{jjy} stiffness accounting for η_A, η_B with respect to y-axis
k_{iiz}, k_{ijz}, k_{jjz} stiffness accounting for η_A, η_B with respect to z-axis
L_b unbraced length of the member in the out-of-plane bending
L_c length of column accounting for geometric imperfection
L_p limiting unbraced length for full plastic bending capacity
L_r limiting unbraced length of inelastic lateral torsional buckling
M_A absolute value of moment at quarter point of the unbraced segment, sum of moments in sway and non-sway cases
M_B absolute value of moment at centerline of the unbraced segment, sum of moments in sway and non-sway cases
M_C absolute value of moment at three quarter point of the unbraced segment, sum of moments in sway and non-sway cases
M_{max} absolute value of maximum moment in the unbraced segment, sum of moments in sway and non-sway cases
M_n lateral torsional buckling strength
M_r $F_L S_x$, where F_L is smaller of $(F_{yf} - F_r)$ or F_{yw}
M_y, M_z second-order bending moment with respect to y- and z-axes
M_{yp}, M_{zp} plastic moment capacity with respect to y- and z-axes
M_p plastic moment capacity
M_{yA}, M_{yB}, M_{zA}, M_{zB} end moments with respect to y- and z-axes
P second-order axial force or axial force
P_y squash load
P_p axially ultimate load
r_1, r_2 factors which account for the length and number of columns
r_y radius of gyration about y-axis
S_x section modulus about x-axis
S_1, S_2, S_3, S_4 stability functions with respect to y- and z-axes
T torsional force
α force-state parameter
δ axial shortening

η, η_A, η_B stiffness degradation function at element end A and B, respectively
θ_{yA}, θ_{yB}, θ_{zA}, θ_{zB} the joint rotations
ϕ the angle of twist

perhaps the most serious limitation is probably the rationale of the current two-stage process in design: elastic analysis is used to determine the forces acting on each member of a structural system, whereas inelastic analysis is used to determine the strength of each member treated as an isolated member. There is no verification of the compatibility between the isolated member and the member as part of a frame. The individual member strength equations as specified in specifications are unconcerned with system compatibility. As a result, there is no explicit guarantee that all members will sustain their design loads under the geometric configuration imposed by the framework.

In order to overcome the difficulties of the conventional approach, second-order plastic-hinge analysis should be directly performed. With the current available computing technology with advancement in computer hardware and software, it is feasible to employ second-order plastic-hinge analysis techniques for direct frame design. Most of second-order plastic analyses can be categorized into one of two types: (1) plastic zone; or (2) plastic hinge based on the degree of refinements used to represent yielding. The plastic-zone method uses the highest refinements while the elastic–plastic hinge method allows for significant simplifications. The typical load–displacements of the plastic analyses are illustrated in Fig. 1. One of the second-order plastic-hinge analyses called the plastic-zone method discretizes frame members into several finite elements. Also the cross-section of each finite element is further subdivided into many fibers (Vogel, 1985; White, 1985; Clarke et al., 1992). Although the plastic-zone solution is known as an "exact solution", it is yet to be used for practical design purposes. The applicability of the method is limited by its complexity requiring intensive computational time and cost. The real challenge in our endeavor is to make this type of analysis competitive in present construction engineering practices.

A more simple and efficient way to represent inelasticity in frames is the second-order plastic-hinge method. Until now, several second-order plastic-hinge analyses for space structures were developed by Ziemian et al. (1992), Prakash and Powell (1993), Liew and Tang (1998), and Kim et al. (2001). The benefit of the second-order plastic-hinge analyses is that they are efficient and sufficiently accurate for the assessment of strength and stability of structural systems and their component members.

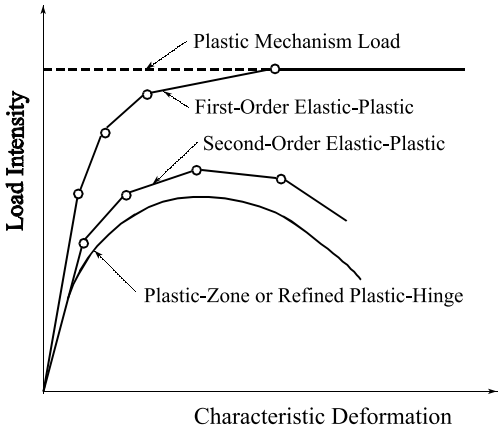

Fig. 1. Load–displacement of plastic analyses.

These conventional 3-D second-order plastic-hinge analyses assume lateral torsional buckling to be prevented by adequate lateral bracing, and do not account for the degradation of the flexural strength caused by lateral torsional buckling. Since the sections of the structures are not always provided with a sufficient lateral support, the analysis should be improved to consider lateral torsional buckling. When the conventional 3-D second-order plastic-hinge analyses account for lateral torsional buckling, it must be a considerable contribution in present engineering practices. The objective of this paper is to achieve the accuracy of a plastic-zone solution with the ease of the plastic-hinge model, in capturing the effect of lateral torsional buckling.

2. 3-D second-order plastic-hinge analysis

2.1. Stability functions accounting for second-order effect

To capture second-order (large displacement) effects, stability functions are used to minimize modeling and solution time. Generally only one or two elements are needed per a member. The simplified stability functions for the two-dimensional beam-column element were reported by Chen and Lui (1992). The force–displacement equation using the stability functions may be extended for three-dimensional beam-column element as

$$\begin{Bmatrix} P \\ M_{y\mathrm{A}} \\ M_{y\mathrm{B}} \\ M_{z\mathrm{A}} \\ M_{z\mathrm{B}} \\ T \end{Bmatrix} = \begin{bmatrix} \frac{EA}{L} & 0 & 0 & 0 & 0 & 0 \\ 0 & S_1\frac{EI_y}{L} & S_2\frac{EI_y}{L} & 0 & 0 & 0 \\ 0 & S_2\frac{EI_y}{L} & S_1\frac{EI_y}{L} & 0 & 0 & 0 \\ 0 & 0 & 0 & S_3\frac{EI_z}{L} & S_4\frac{EI_z}{L} & 0 \\ 0 & 0 & 0 & S_4\frac{EI_z}{L} & S_3\frac{EI_z}{L} & 0 \\ 0 & 0 & 0 & 0 & 0 & \frac{GJ}{L} \end{bmatrix} \begin{Bmatrix} \delta \\ \theta_{y\mathrm{A}} \\ \theta_{y\mathrm{B}} \\ \theta_{z\mathrm{A}} \\ \theta_{z\mathrm{B}} \\ \phi \end{Bmatrix} \tag{1}$$

where P is the axial force; $M_{y\mathrm{A}}$, $M_{y\mathrm{B}}$, $M_{z\mathrm{A}}$, $M_{z\mathrm{B}}$, the end moments with respect to y- and z-axes; T, the torsional force; δ, the axial shortening; $\theta_{y\mathrm{A}}$, $\theta_{y\mathrm{B}}$, $\theta_{z\mathrm{A}}$, $\theta_{z\mathrm{B}}$, the joint rotations; ϕ, the angle of twist; S_1, S_2, S_3, S_4, the stability functions with respect to y- and z-axes; A, L, the area and length of beam-column element; I_y, I_z, the moment of inertia with respect to y- and z-axes; E, the modulus of elasticity; G, the shear modulus of elasticity; J, the torsional constant.

The stability functions given by Eq. (1) may be written as

$$S_1 = \begin{cases} \dfrac{\pi\sqrt{\rho_y}\sin(\pi\sqrt{\rho_y}) - \pi^2\rho_y\cos(\pi\sqrt{\rho_y})}{2 - 2\cos(\pi\sqrt{\rho_y}) - \pi\sqrt{\rho_y}\sin(\pi\sqrt{\rho_y})} & \text{if } P < 0 \\ \dfrac{\pi^2\rho_y\cosh(\pi\sqrt{\rho_y}) - \pi\sqrt{\rho_y}\sinh(\pi\sqrt{\rho_y})}{2 - 2\cosh(\pi\sqrt{\rho_y}) + \pi\sqrt{\rho_y}\sinh(\pi\sqrt{\rho_y})} & \text{if } P > 0 \end{cases} \tag{2a}$$

$$S_2 = \begin{cases} \dfrac{\pi^2\rho_y - \pi\sqrt{\rho_y}\sin(\pi\sqrt{\rho_y})}{2 - 2\cos(\pi\sqrt{\rho_y}) - \pi\sqrt{\rho_y}\sin(\pi\sqrt{\rho_y})} & \text{if } P < 0 \\ \dfrac{\pi\sqrt{\rho_y}\sinh(\pi\sqrt{\rho_y}) - \pi^2\rho_y}{2 - 2\cosh(\pi\sqrt{\rho_y}) + \pi\sqrt{\rho_y}\sin(\pi\sqrt{\rho_y})} & \text{if } P > 0 \end{cases} \tag{2b}$$

$$S_3 = \begin{cases} \dfrac{\pi\sqrt{\rho_z}\sin(\pi\sqrt{\rho_z}) - \pi^2\rho_z\cos(\pi\sqrt{\rho_z})}{2 - 2\cos(\pi\sqrt{\rho_z}) - \pi\sqrt{\rho_z}\sin(\pi\sqrt{\rho_z})} & \text{if } P < 0 \\ \dfrac{\pi^2\rho\cosh(\pi\sqrt{\rho_z}) - \pi\sqrt{\rho_z}\sinh(\pi\sqrt{\rho_z})}{2 - 2\cosh(\pi\sqrt{\rho_z}) + \pi\sqrt{\rho_z}\sinh(\pi\sqrt{\rho_z})} & \text{if } P > 0 \end{cases} \tag{2c}$$

$$S_4 = \begin{cases} \dfrac{\pi^2\rho_z - \pi\sqrt{\rho_z}\sin(\pi\sqrt{\rho_z})}{2 - 2\cos(\pi\sqrt{\rho_z}) - \pi\sqrt{\rho_z}\sin(\pi\sqrt{\rho_z})} & \text{if } P < 0 \\ \dfrac{\pi\sqrt{\rho_z}\sinh(\pi\sqrt{\rho_z}) - \pi^2\rho_z}{2 - 2\cosh(\pi\sqrt{\rho_z}) + \pi\sqrt{\rho_z}\sin(\pi\sqrt{\rho_z})} & \text{if } P > 0 \end{cases} \tag{2d}$$

where $\rho_y = P/(\pi^2 EI_y/L^2)$, $\rho_z = P/(\pi^2 EI_z/L^2)$, and P is positive in tension.

The numerical solutions obtained from Eqs. (2a)–(2d) are indeterminate when the axial force is zero. To circumvent this problem and to avoid the use of different expressions for S_1, S_2, S_3, and S_4 for a different sign of axial forces, Lui and Chen (1986) have proposed a set of expressions that make use of power-series expansions to approximate the stability functions. The power-series expressions have been shown to converge to a high degree of accuracy within the first 10 terms of the series expansions. Alternatively, if the axial force in the member falls within the range $-2.0 \leqslant \rho \leqslant 2.0$, the following simplified expressions may be used to closely approximate the stability functions:

$$S_1 = 4 + \frac{2\pi^2\rho_y}{15} - \frac{(0.01\rho_y + 0.543)\rho_y^2}{4 + \rho_y} - \frac{(0.004\rho_y + 0.285)\rho_y^2}{8.183 + \rho_y} \tag{3a}$$

$$S_2 = 2 - \frac{\pi^2\rho_y}{30} + \frac{(0.01\rho_y + 0.543)\rho_y^2}{4 + \rho_y} - \frac{(0.004\rho_y + 0.285)\rho_y^2}{8.183 + \rho_y} \tag{3b}$$

$$S_3 = 4 + \frac{2\pi^2\rho_z}{15} - \frac{(0.01\rho_z + 0.543)\rho_z^2}{4 + \rho_z} - \frac{(0.004\rho_z + 0.285)\rho_z^2}{8.183 + \rho_z} \tag{3c}$$

$$S_4 = 2 - \frac{\pi^2\rho_z}{30} + \frac{(0.01\rho_z + 0.543)\rho_z^2}{4 + \rho_z} - \frac{(0.004\rho_z + 0.285)\rho_z^2}{8.183 + \rho_z} \tag{3d}$$

Eqs. (3a)–(3d) are applicable for members in tension (positive P) and compression (negative P). For most practical applications, Eqs. (3a)–(3d) give an excellent correlation to the exact expressions given by Eqs. (2a)–(2d). However, for ρ other than the range of $-2.0 \leqslant \rho \leqslant 2.0$, the conventional stability functions (Eqs. (2a)–(2d)) should be used. The stability function approach uses only one element per member and maintains accuracy in the element stiffness terms and in the recovery of element end forces for all ranges of axial loads. In this formulation, all members are assumed to be adequately braced to prevent out-of-plane buckling, and their cross-sections are compact.

2.2. Plastic strength of cross-section

Based on the AISC-load and resistance factor design (LRFD) bilinear interaction equations, a cross-section's plastic strength can be taken as (AISC, 1993)

$$\left|\frac{P}{P_p}\right| + \frac{8}{9}\left|\frac{M_y}{M_{yp}}\right| + \frac{8}{9}\left|\frac{M_z}{M_{zp}}\right| = 1.0 \quad \text{for } \frac{P}{P_p} \geqslant 0.2 \tag{4a}$$

$$\left|\frac{P}{2P_p}\right| + \left|\frac{M_y}{M_{yp}}\right| + \left|\frac{M_z}{M_{zp}}\right| = 1.0 \quad \text{for } \frac{P}{P_p} < 0.2 \tag{4b}$$

where P is the second-order axial force; P_p, the axially ultimate load; M_y, M_z, the second-order bending moment with respect to y- and z-axes; M_{yp}, M_{zp}, the plastic moment capacity with respect to y- and z-axes.

The strain is not involved in this analysis. Once the member forces get to the full plastic surface given by Eqs. (4a) and (4b), they are assumed to move on the plastic surface at the following loading step. That is,

once the axial force of a member increases at the following loading step, the bending moment is adjusted to be reduced. Thus, the member forces do not violate the yield surface. This approach has been used by several researchers (Chen and Kim, 1997; Kim and Chen, 1996a, 1996b; Liew et al., 1993).

2.3. Model for gradual yielding

A lot of meshes are necessary in order to trace the inelastic stress–strain relationship of each fine element (Ilyushin, 1956). The approach is widely used in the commercial softwares including ABAQUS, ANSYS, and etc. Those softwares are good at research purpose but not at design use. Since the purpose of this paper is to develop a practical tool for at design use, the plasticity is approximated by using the column research council (CRC) and the parabolic function whose values are determined by member forces rather than by stress and strain relationship of each mesh. Although this approximation is used, the method predicts the system strength with a reasonable accuracy as shown in the verification study. This approach has been developed and used by many researchers (Liew and Tang, 1998; Chen and Kim, 1997; Kim and Chen, 1996a, 1996b; Clarke et al., 1992; Orbison 1982).

2.3.1. Column research council tangent modulus model associated with residual stresses

The CRC tangent modulus concept is used to account for gradual yielding (due to residual stresses) along the length of axially loaded members between plastic hinges (Chen and Lui, 1992). The elastic modulus E, instead of moment of inertia I, is hereby reduced. Although it is really the elastic portion of the cross-section (thus I) that is being reduced, changing the elastic modulus is easier than changing the moment of inertia for different sections. The rate of reduction in stiffness is different in the weak and strong directions, but this is not considered since the dramatic degradation of weak-axis stiffness is compensated for by the substantial weak-axis' plastic strength (Chen and Kim, 1997). This simplification makes the present methods practical. From Chen and Lui (1992), the CRC E_t is written as

$$E_t = 1.0E \qquad \text{for } P \leqslant 0.5P_y \tag{5a}$$

$$E_t = 4\frac{P}{P_y}E\left(1-\frac{P}{P_y}\right) \quad \text{for } P > 0.5P_y \tag{5b}$$

2.3.2. Parabolic function for gradual yielding due to flexure

The tangent modulus model is suitable for the member subjected to axial force, but not adequate for cases of both axial force and bending moment. A gradual stiffness degradation model for a plastic hinge is required to represent the partial plastification effects associated with bending. When softening plastic hinges are active at both ends of an element, the force–deflection equation may be expressed as

$$\begin{Bmatrix} P \\ M_{y\mathrm{A}} \\ M_{y\mathrm{B}} \\ M_{z\mathrm{A}} \\ M_{z\mathrm{B}} \\ T \end{Bmatrix} = \begin{bmatrix} \frac{E_t A}{L} & 0 & 0 & 0 & 0 & 0 \\ 0 & k_{iiy} & k_{ijy} & 0 & 0 & 0 \\ 0 & k_{ijy} & k_{jjy} & 0 & 0 & 0 \\ 0 & 0 & 0 & k_{iiz} & k_{ijz} & 0 \\ 0 & 0 & 0 & k_{ijz} & k_{jjz} & 0 \\ 0 & 0 & 0 & 0 & 0 & \eta_{\mathrm{A}}\eta_{\mathrm{B}}\frac{GJ}{L} \end{bmatrix} \begin{Bmatrix} \delta \\ \theta_{y\mathrm{A}} \\ \theta_{y\mathrm{B}} \\ \theta_{z\mathrm{A}} \\ \theta_{z\mathrm{B}} \\ \phi \end{Bmatrix} \tag{6}$$

where

$$k_{iiy} = \eta_{\mathrm{A}}\left(S_1 - \frac{S_2^2}{S_1}(1-\eta_{\mathrm{B}})\right)\frac{E_t I_y}{L} \tag{7a}$$

$$k_{ijy} = \eta_A \eta_B S_2 \frac{E_t I_y}{L} \tag{7b}$$

$$k_{jjy} = \eta_B \left(S_1 - \frac{S_2^2}{S_1}(1-\eta_A) \right) \frac{E_t I_y}{L} \tag{7c}$$

$$k_{iiz} = \eta_A \left(S_3 - \frac{S_4^2}{S_3}(1-\eta_B) \right) \frac{E_t I_z}{L} \tag{7d}$$

$$k_{ijz} = \eta_A \eta_B S_4 \frac{E_t I_z}{L} \tag{7e}$$

$$k_{jjz} = \eta_B \left(S_3 - \frac{S_4^2}{S_3}(1-\eta_A) \right) \frac{E_t I_z}{L} \tag{7f}$$

The terms η_A and η_B are scalar parameters that allow for gradual inelastic stiffness reduction of the element associated with plastification at end A and B. This term is equal to 1.0 when the element is elastic, and zero when a plastic hinge is formed. The parameter η is assumed to vary according to the parabolic function:

$$\eta = 1.0 \quad \text{for } \alpha \leqslant 0.5 \tag{8a}$$

$$\eta = 4\alpha(1-\alpha) \quad \text{for } \alpha > 0.5 \tag{8b}$$

where α is a force-state parameter that measures the magnitude of axial force and bending moment at the element end. Herein, α is the function of the AISC-LRFD interaction equations written in Eqs. (9a) and (9b).

$$\alpha = \frac{P}{P_p} + \frac{8}{9}\frac{M_y}{M_{yp}} + \frac{8}{9}\frac{M_z}{M_{zp}} \quad \text{for } \frac{P}{P_p} \geqslant \frac{2}{9}\frac{M_y}{M_{yp}} + \frac{2}{9}\frac{M_z}{M_{zp}} \tag{9a}$$

$$\alpha = \frac{P}{2P_p} + \frac{M_y}{M_{yp}} + \frac{M_z}{M_{zp}} \quad \text{for } \frac{P}{P_p} < \frac{2}{9}\frac{M_y}{M_{yp}} + \frac{2}{9}\frac{M_z}{M_{zp}} \tag{9b}$$

Initial yielding is assumed to occur based on a yield surface that has the same shape as the full plastification surface and with the force-state parameter denoted as $\alpha_0 = 0.5$. If the forces change so the force point moves inside or along the initial yield surface, the element is assumed to remain fully elastic with no stiffness reduction. If the force point moves beyond the initial yield surface, the element stiffness is reduced to account for the effect of plastification at the element end.

The element force–displacement relationship from Eq. (6) may be symbolically written as

$$\{f_e\} = [K_e]\{d_e\} \tag{10}$$

in which $\{f_e\}$ and $\{d_e\}$ are the element end force and displacement arrays, and $[K_e]$ is the element tangent stiffness matrix.

To account for transverse shear deformation effects in a beam-column element, the stiffness matrix may be modified as

$$\begin{Bmatrix} P \\ M_{yA} \\ M_{yB} \\ M_{zA} \\ M_{zB} \\ T \end{Bmatrix} = \begin{bmatrix} \frac{E_t A}{L} & 0 & 0 & 0 & 0 & 0 \\ 0 & C_{iiy} & C_{ijy} & 0 & 0 & 0 \\ 0 & C_{ijy} & C_{jjy} & 0 & 0 & 0 \\ 0 & 0 & 0 & C_{iiz} & C_{ijz} & 0 \\ 0 & 0 & 0 & C_{ijz} & C_{jjz} & 0 \\ 0 & 0 & 0 & 0 & 0 & \eta_A \eta_B \frac{GJ}{L} \end{bmatrix} \begin{Bmatrix} \delta \\ \theta_{yA} \\ \theta_{yB} \\ \theta_{zA} \\ \theta_{zB} \\ \phi \end{Bmatrix} \tag{11}$$

where

$$C_{iiy} = \frac{k_{iiy}k_{jjy} - k_{ijy}^2 + k_{iiy}A_{sz}GL}{k_{iiy} + k_{jjy} + 2k_{ijy} + A_{sz}GL} \tag{12a}$$

$$C_{ijy} = \frac{-k_{iiy}k_{jjy} + k_{ijy}^2 + k_{ijy}A_{sz}GL}{k_{iiy} + k_{jjy} + 2k_{ijy} + A_{sz}GL} \tag{12b}$$

$$C_{jjy} = \frac{k_{iiy}k_{jjy} - k_{ijy}^2 + k_{jjy}A_{sz}GL}{k_{iiy} + k_{jjy} + 2k_{ijy} + A_{sz}GL} \tag{12c}$$

$$C_{iiz} = \frac{k_{iiz}k_{jjz} - k_{ijz}^2 + k_{iiz}A_{sy}GL}{k_{iiz} + k_{jjz} + 2k_{ijz} + A_{sy}GL} \tag{12d}$$

$$C_{ijz} = \frac{-k_{iiz}k_{jjz} + k_{ijz}^2 + k_{ijz}A_{sy}GL}{k_{iiz} + k_{jjz} + 2k_{ijz} + A_{sy}GL} \tag{12e}$$

$$C_{jjz} = \frac{k_{iiz}k_{jjz} - k_{ijz}^2 + k_{jjz}A_{sy}GL}{k_{iiz} + k_{jjz} + 2k_{ijz} + A_{sy}GL} \tag{12f}$$

2.4. Stability analysis of structural system

The end forces and end displacements used in Eq. (10) are shown in Fig. 2(a). The sign convention for the positive directions of element end forces and end displacements of a frame member is shown in

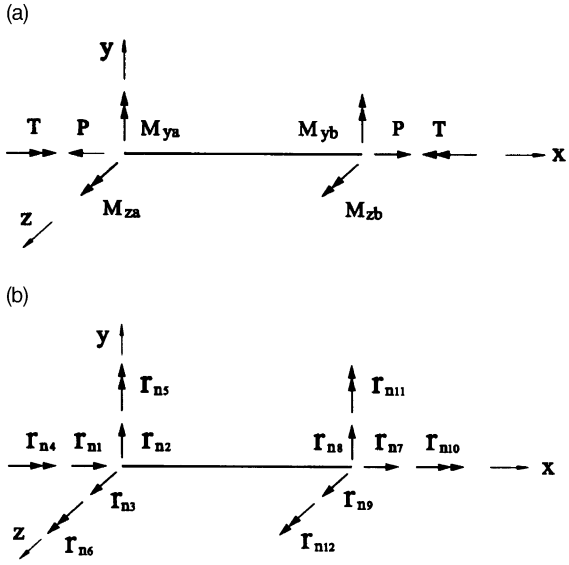

Fig. 2. Element end forces and displacements notation.

Fig. 2(b). By comparing the two figures, we can express the equilibrium and kinematic relationships in symbolic form as

$$\{f_n\} = [T]^{\mathrm{T}}_{6\times12}\{f_{\mathrm{e}}\} \tag{13a}$$

$$\{d_{\mathrm{e}}\} = [T]_{6\times12}\{d_L\} \tag{13b}$$

$\{f_n\}$ and $\{d_L\}$ are the end force and displacement vectors of a frame member expressed as

$$\{f_n\}^{\mathrm{T}} = \{\, r_{n1} \quad r_{n2} \quad r_{n3} \quad r_{n4} \quad r_{n5} \quad r_{n6} \quad r_{n7} \quad r_{n8} \quad r_{n9} \quad r_{n10} \quad r_{n11} \quad r_{n12} \,\} \tag{14a}$$

$$\{d_L\}^{\mathrm{T}} = \{\, d_1 \quad d_2 \quad d_3 \quad d_4 \quad d_5 \quad d_6 \quad d_7 \quad d_8 \quad d_9 \quad d_{10} \quad d_{11} \quad d_{12} \,\} \tag{14b}$$

$\{f_{\mathrm{e}}\}$ and $\{d_{\mathrm{e}}\}$ are the end force and displacement vectors in Eq. (10). $[T]_{6\times12}$ is a transformation matrix written as

$$[T]_{6\times12} = \begin{bmatrix} -1 & 0 & 0 & 0 & 0 & 0 & 1 & 0 & 0 & 0 & 0 & 0 \\ 0 & 0 & -\frac{1}{L} & 0 & 1 & 0 & 0 & 0 & \frac{1}{L} & 0 & 0 & 0 \\ 0 & 0 & -\frac{1}{L} & 0 & 0 & 0 & 0 & 0 & \frac{1}{L} & 0 & 1 & 0 \\ 0 & \frac{1}{L} & 0 & 0 & 0 & 1 & 0 & -\frac{1}{L} & 0 & 0 & 0 & 0 \\ 0 & \frac{1}{L} & 0 & 0 & 0 & 0 & 0 & -\frac{1}{L} & 0 & 0 & 0 & 1 \\ 0 & 0 & 0 & 1 & 0 & 0 & 0 & 0 & 0 & -1 & 0 & 0 \end{bmatrix} \tag{15}$$

Using the transformation matrix by equilibrium and kinematic relations, the force–displacement relationship of a frame member may be written as

$$\{f_n\} = [K_n]\{d_L\} \tag{16}$$

$[K_n]$ is the element stiffness matrix expressed as

$$[K_n]_{12\times12} = [T]^{\mathrm{T}}_{6\times12}[K_{\mathrm{e}}]_{6\times6}[T]_{6\times12} \tag{17}$$

Eq. (17) can be subgrouped as

$$[K_n]_{12\times12} = \begin{bmatrix} [K_n]_1 & [K_n]_2 \\ [K_n]_2^{\mathrm{T}} & [K_n]_3 \end{bmatrix} \tag{18}$$

where

$$[K_n]_1 = \begin{bmatrix} a & 0 & 0 & 0 & 0 & 0 \\ 0 & b & 0 & 0 & 0 & c \\ 0 & 0 & d & 0 & -e & 0 \\ 0 & 0 & 0 & f & 0 & 0 \\ 0 & 0 & -e & 0 & g & 0 \\ 0 & c & 0 & 0 & 0 & h \end{bmatrix} \tag{19a}$$

$$[K_n]_2 = \begin{bmatrix} -a & 0 & 0 & 0 & 0 & 0 \\ 0 & -b & 0 & 0 & 0 & c \\ 0 & 0 & -d & 0 & -e & 0 \\ 0 & 0 & 0 & -f & 0 & 0 \\ 0 & 0 & e & 0 & i & 0 \\ 0 & -c & 0 & 0 & 0 & j \end{bmatrix} \tag{19b}$$

$$[K_n]_3 = \begin{bmatrix} a & 0 & 0 & 0 & 0 & 0 \\ 0 & b & 0 & 0 & 0 & -c \\ 0 & 0 & d & 0 & e & 0 \\ 0 & 0 & 0 & f & 0 & 0 \\ 0 & 0 & e & 0 & m & 0 \\ 0 & c & 0 & 0 & 0 & n \end{bmatrix} \tag{19c}$$

where

$$a = \frac{E_t A}{L}, \quad b = \frac{C_{iiz} + 2C_{ijz} + C_{jjz}}{L^2}, \quad c = \frac{C_{iiz} + C_{ijz}}{L}, \quad d = \frac{C_{iiy} + 2C_{ijy} + C_{jjy}}{L^2}, \quad e = \frac{C_{iiy} + C_{ijy}}{L},$$
$$f = \frac{GJ}{L}, \quad g = C_{iiy}, \quad h = C_{iiz}, \quad i = C_{ijy}, \quad j = C_{ijz}, \quad m = C_{jjy}, \quad n = C_{jjz} \tag{20}$$

Eq. (18) is used to enforce no sidesway in the member. If the member is permitted to sway, an additional axial and shear forces will be induced in the member. We can relate this additional axial and shear forces due to a member sway to the member end displacements as

$$\{f_s\} = [K_s]\{d_L\} \tag{21}$$

where $\{f_s\}$, $\{d_L\}$, and $[K_s]$ are end force vector, end displacement vector, and the element stiffness matrix. They may be written as

$$\{f_s\}^T = \{\, r_{s1} \quad r_{s2} \quad r_{s3} \quad r_{s4} \quad r_{s5} \quad r_{s6} \quad r_{s7} \quad r_{s8} \quad r_{s9} \quad r_{s10} \quad r_{s11} \quad r_{s12} \,\} \tag{22a}$$

$$\{d_L\}^T = \{\, d_1 \quad d_2 \quad d_3 \quad d_4 \quad d_5 \quad d_6 \quad d_7 \quad d_8 \quad d_9 \quad d_{10} \quad d_{11} \quad d_{12} \,\} \tag{22b}$$

$$[K_s]_{12\times 12} = \begin{bmatrix} [K_s] & -[K_s] \\ -[K_s]^T & [K_s] \end{bmatrix} \tag{22c}$$

where

$$[K_s] = \begin{bmatrix} 0 & a & -b & 0 & 0 & 0 \\ a & c & 0 & 0 & 0 & 0 \\ -b & 0 & c & 0 & 0 & 0 \\ 0 & 0 & 0 & 0 & 0 & 0 \\ 0 & 0 & 0 & 0 & 0 & 0 \\ 0 & 0 & 0 & 0 & 0 & 0 \end{bmatrix} \tag{23}$$

and

$$a = \frac{M_{zA} + M_{zB}}{L^2}, \quad b = \frac{M_{yA} + M_{yB}}{L^2}, \quad c = \frac{P}{L} \tag{24}$$

By combining Eqs. (16) and (21), we obtain the general beam-column element force–displacement relationship as

$$\{f_L\} = [K]_{\text{local}}\{d_L\} \tag{25}$$

where

$$\{f_L\} = \{f_n\} + \{f_s\} \tag{26}$$

$$[K]_{\text{local}} = [K_n] + [K_s] \tag{27}$$

We need to transform the elemental stiffness matrix with respect to the elemental coordinate system to the global coordinate system before combining the stiffnesses to create the structural stiffness matrix. The basic form of this transformation is shown in Eq. (28).

$$[K]_{\text{global}} = [\beta]^{\text{T}}[K]_{\text{local}}[\beta] \tag{28}$$

The elements of $[\beta]$ matrix were the direction cosines of the force and displacement vectors. For the force and displacement vectors. For the three-dimensional frame element the $[\beta]$ matrix expands to

$$[\beta] = \begin{bmatrix} [L] & 0 & 0 & 0 \\ 0 & [L] & 0 & 0 \\ 0 & 0 & [L] & 0 \\ 0 & 0 & 0 & [L] \end{bmatrix} \tag{29}$$

where each $[L]$ matrix is the 3×3 matrix of direction cosines.

2.5. Geometric imperfection modeling

2.5.1. Braced frame

The proposed analysis implicitly accounts for the effects of both residual stresses and spread of yielded zones. To this end, proposed analysis may be regarded as equivalent to the plastic-zone analysis. As a result, geometric imperfections are necessary only to consider fabrication error. For braced frames, member out-of-straightness, rather than frame out-of-plumbness, needs to be used for geometric imperfections. This is because the P–Δ effect due to the frame out-of-plumbness is diminished by braces. The ECCS (1984, 1991), AS (1990), and CSA (1989, 1994) specifications recommend an initial crookedness of column equal to 1/1000 times the column length. The AISC code recommends the same maximum fabrication tolerance of $L_c/1000$ for member out-of-straightness. In this study, a geometric imperfection of $L_c/1000$ is adopted.

The ECCS, AS, and CSA specifications recommend the out-of-straightness varying sinusoidally with a maximum in-plane deflection at the mid-height. They do not, however, describe how the sinusoidal imperfection should be modeled in analysis. Ideally, many elements are needed to model the sinusoidal out-of-straightness of a beam-column member, but it is not practical. In this study, two elements with a maximum initial deflection at the mid-height of a member are found adequate for capturing the imperfection. Fig. 3 shows the out-of-straightness modeling for a braced beam-column member. It may be observed that the out-of-plumbness is equal to 1/500 when the half segment of the member is considered. This value is

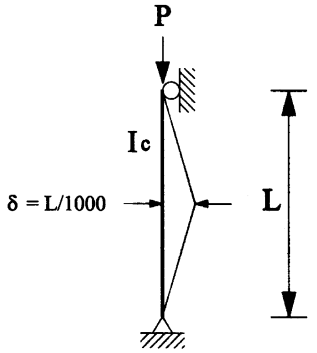

Fig. 3. Explicit imperfection modeling of braced member.

identical to that of sway frames as discussed in recent papers by Kim and Chen (1996a, 1996b). Thus, it may be stated that the imperfection values are essentially identical for both sway and braced frames.

2.5.2. Unbraced frame

Referring to the European Convention for Constructional Steelwork (ECCS, 1984, 1991), an out-of-plumbness of a column equal to 1/200 times the column height is recommended for the elastic plastic-hinge analysis. For multi-story and multi-bay frames, the geometric imperfections may be reduced to $1/200k_ck_s$ since all columns in buildings may not lean in the same direction. The coefficients, k_c and k_s account for the situation where a large number of columns in a story and stories in a frame would reduce the total magnitude of geometric imperfections. According to the ECCS (1984, 1991), the member initial out-of-straightness should be modeled at the same time with the initial out-of-plumbness if the column parameter $L\sqrt{P_u/EI}$ is larger than 1.6. This may be necessary to consider residual stresses and possible member instability effects for highly compressed slender columns, however, the magnitude of the imperfection is not specified in the ECCS (1984, 1991).

Since plastic-zone analysis accounts for both residual stresses and the spread of yielding, only geometric imperfections for erection tolerances need be included in the analysis. The ECCS recommends the out-of-plumbness of columns equal to $1/300r_1r_2$ times the column height where r_1 and r_2 are factors which account for the length and number of columns, respectively. For the plastic-zone analysis, the ECCS does not specify the requirement of the initial out-of-straightness to be modeled in addition to the out-of-plumbness when the column parameter $L\sqrt{P_u/EI}$ is larger than 1.6, since the plastic-zone analysis already includes residual stresses and spread of yielding in its formulation.

Since proposed analysis implicitly accounts for both residual stresses and the spread of yielding, it may be considered equivalent to the plastic-zone analysis. Thus, modeling the out-of-plumbness for erection tolerances is used here without the out-of-straightness for the column, regardless of the value of the column parameter, so that the same ultimate strength can be predicted for mathematically identical braced and unbraced members. This simplification enables us to use the proposed methods easily with consistent imperfection modeling. The Canadian Standard (1989, 1994) and the AISC Code of Standard Practice (AISC, 1994) set the limit of erection out-of-plumbness $L_c/500$. The maximum erection tolerances in the AISC are limited to 1 in. toward the exterior of buildings and 2 in. toward the interior of buildings less than 20 stories. Considering the maximum permitted average lean of 1.5 in. in the same direction of a story, the geometric imperfection of $L_c/500$ can be used for buildings up to six stories with each story approximately 10 feet high. For taller buildings, this imperfection value of $L_c/500$ is conservative since the accumulated geometric imperfection calculated by 1/500 times building height is greater than the maximum permitted erection tolerance.

In this study, we shall use $L_c/500$ for the out-of-plumbness without any modification because the system strength is often governed by a weak story which has an out-of-plumbness equal to $L_c/500$ (Maleck et al., 1995) and a constant imperfection has the benefit of simplicity in practical design. The explicit geometric imperfection modeling for an unbraced frame is illustrated in Fig. 4.

3. Model to account for lateral torsional buckling

When a member is bent about its major axis, out-of-plane motion consisting of bending and twisting will occur as the applied load increases. The out-of-plane motion results in the degradation of the flexural strength and stiffness about its major axis. The conventional 3-D second-order plastic-hinge analyses, however, do not consider the degradation of the flexural strength caused by the lateral torsional buckling, assuming the lateral torsional motion to be prevented by adequate lateral bracing. The analysis should be

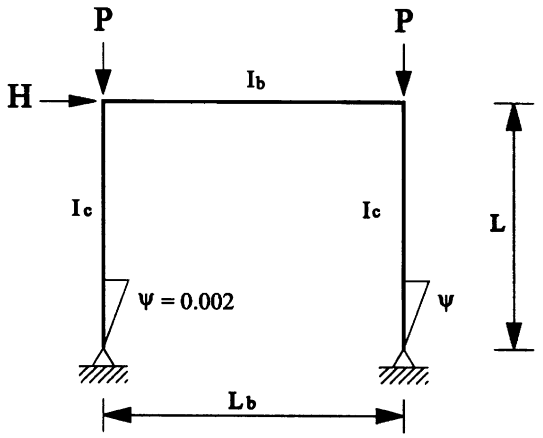

Fig. 4. Explicit imperfection modeling of unbraced frame.

improved to consider lateral torsional buckling, since the real structures are not always provided with a sufficient lateral support.

A theoretical model was developed for the inelastic lateral torsional buckling of beams under uniform moment (Kitipornchai and Trahair, 1974). The inelastic lateral torsional buckling of steel I-beams under moment gradient was studied theoretically (Kitipornchai and Trahair, 1975). A number of full-scale tests on steel I-beams were made by Hechtman et al. (1995), White (1960), and Sawer (1961) among many others.

The unbraced length, the cross-sectional shape, and the material property are the important factors influencing the lateral torsional buckling strength. Since the 3-D second-order plastic-hinge analysis uses only a line model to represent an element, a rigorous model using volume elements to account for lateral torsional effect is not applicable to this analysis. In this study, the practical LRFD equation among Rondal and Maquoi (1979), ECCS (1991), and AISC (1994) is used to determine the lateral torsional buckling strength.

For I-shaped members subjected to bending about the strong-axis, M_n is determined by:

$$M_n = M_p \quad \text{for } L_b \leqslant L_p \tag{30a}$$

$$M_n = C_b\left[M_p - (M_p - M_r)\frac{(L_b - L_p)}{(L_r - L_p)}\right] \leqslant M_p \quad \text{for } L_p < L_b \leqslant L_r \tag{30b}$$

$$M_n = C_b\frac{\pi}{L_b}\sqrt{EI_yGJ + \left(\frac{\pi E}{L_b}\right)^2 I_yC_w} \leqslant C_bM_r \quad \text{for } L_b > L_r \tag{30c}$$

where M_p is the plastic moment $= F_yZ$, where Z is plastic section modulus; M_r, the F_LS_x, where F_L is smaller of $(F_{yf} - F_r)$ or F_{yw}; F_{yf}, the yield stress of flange; F_{yw}, the yield stress of web; F_r, the compressive residual stress in flange; 10 ksi for rolled shape, 16.5 ksi for welded shape; L_b, the unbraced length of the member in the out-of-plane bending; L_p, the limiting unbraced length for full plastic bending capacity; L_r, the limiting unbraced length of inelastic lateral torsional buckling; I_y, the moment of inertia about weak axis; G, the shear modulus of elasticity of steel (11,200 ksi); J, the torsional constant; C_w, the warping constant.

The limiting unbraced plastic and elastic lengths (L_p and L_r) shall be determined respectively as follows:

$$L_p = \frac{300 r_y}{\sqrt{F_{yf}}} \tag{31}$$

$$L_r = \frac{r_y X_1}{F_L}\sqrt{1+\sqrt{1+X_2 F_L^2}} \tag{32}$$

where

$$X_1 = \frac{\pi}{S_x}\sqrt{\frac{EGJA}{2}}$$

$$X_2 = 4\frac{C_w}{I_y}\left(\frac{S_x}{GJ}\right)^2$$

S_x is the section modulus about major axis.

It is noted that the lateral torsional buckling limit state is applicable to members subject to strong-axis bending not weak-axis bending, square or circular shapes. The term M_p, M_r, L_p, and L_r may be found with the aid of beam design table in the AISC-LRFD specification without using Eqs. (9a)–(11) described above. C_b is a modification for non-uniform moment diagrams. The physical meaning of C_b is that it represents the amount of an increase in load-carrying capacity when compared with the critical uniform loading case. An empirical formula for C_b is expressed as (AISC, 1993)

$$C_b = \frac{12.5 M_{max}}{2.5 M_{max} + 3M_A + 4M_B + 3M_C} \tag{33}$$

where M_{max} is the absolute value of maximum moment in the unbraced segment, sum of moments in sway and non-sway cases; M_A, the absolute value of moment at quarter point of the unbraced segment, sum of moments in sway and non-sway cases; M_B, the absolute value of moment at centerline of the unbraced segment, sum of moments in sway and non-sway cases; M_C, the absolute value of moment at three quarter point of the unbraced segment, sum of moments in sway and non-sway cases.

When $L_b \leqslant L_p$, the full plastic moment will be developed in the section. When $L_p < L_b \leqslant L_r$, inelastic lateral buckling may occur. When $L_b > L_r$, elastic lateral buckling may occur. The plastic moment M_p of Eqs. (4a) and (4b) is replaced with the lateral torsional buckling strength M_n determined by Eqs. (30a)–(30c). Eqs. (4a) and (4b) are revised as

$$\left|\frac{P}{P_p}\right| + \frac{8}{9}\left|\frac{M_y}{M_{yp}}\right| + \frac{8}{9}\left|\frac{M_z}{M_n}\right| = 1.0 \quad \text{for } \frac{P}{P_p} \geqslant 0.2 \tag{34a}$$

$$\left|\frac{P}{2P_p}\right| + \left|\frac{M_y}{M_{yp}}\right| + \left|\frac{M_z}{M_n}\right| = 1.0 \quad \text{for } \frac{P}{P_p} < 0.2 \tag{34b}$$

Using Eqs. (34a) and (34b) in the 3-D second-order plastic-hinge analysis program, the effect of lateral torsional buckling can be considered. The proposed analysis allows the inelastic moment redistribution in the structural system. Thus, adequate rotational capacity is required. This is achieved when members are adequately braced and their cross-sections are compact. When a member without adequate braces fails by lateral torsional buckling, the moment of inertia of the member is assumed to be zero so that the inelastic moment redistribution is not allowed for the member. This approximation is deemed appropriate for tracing the nonlinear behavior of the frame including lateral torsional buckling effect, since the proposed analysis aims to determine only the ultimate strength of the whole structural system rather than to examine the lateral torsional buckling behavior of a component member.

4. Numerical implementation

Both the simple incremental and the incremental–iteration method are available in the analysis. In the simple incremental method, the applied load increment is automatically reduced to minimize the error when the change in the element stiffness parameter ($\Delta\eta$) exceeds a defined tolerance. In the incremental–iteration load approach, the structure is assumed to behavior linearly at a particular cycle of calculation. Because of the linearization process, equilibrium may be violated and the external force may not always balance the internal force. This unbalance force must be reapplied to the structure. Then, the solution is obtained by iteration process until equilibrium is satisfied. As the stability limit point is approached in the analysis, convergence of the solution may be slow. To facilitate convergence, the applied load increment is automatically reduced. If the structure system is unstable, the determinant of stiffness matrix becomes to either zero or negative value and the program writes "structure unstable".

5. Verification study

Verifications are performed for the following two cases: (1) Orbison's six-story frame ignoring lateral torsional buckling; (2) a single-story frame comprising lateral torsional buckling. The first is to verify how the proposed analysis predicts well geometric and material nonlinear behavior of frames. The second is to show how the proposed analysis captures lateral torsional buckling strength accurately.

5.1. Orbison's six-story space frame ignoring lateral torsional buckling

Fig. 5 shows Orbison's six-story space frame (Orbison, 1982). The yield strength of all members is 250 MPa (36 ksi) and Young's modulus is 206,850 MPa (30,000 ksi). Uniform floor pressure of 4.8 kN/m^2 (100 psf) is converted into equivalent concentrated loads on the top of the columns. Wind loads are simulated by point loads of 26.7 kN (6 kips) in the Y-direction at every beam-column joints.

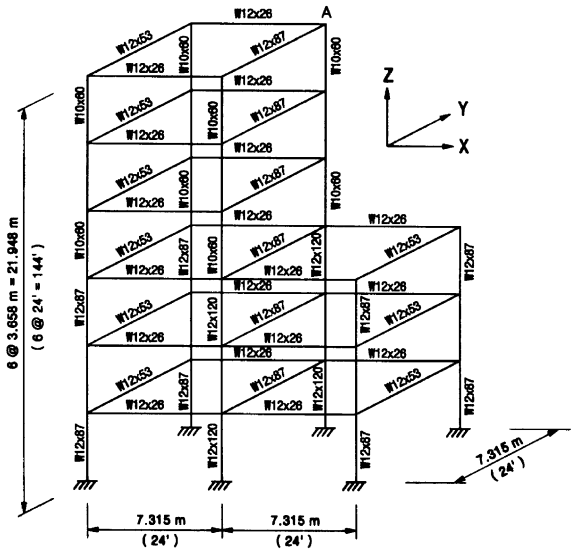

Fig. 5. Six-story space frame.

Table 1
Result of analysis considering shear deformation

Method	Proposed		Liew's
Plastic strength surface	LRFD	Orbison	Orbison
Ultimate load factor	1.990	2.057	2.062
Displacement at A in Y-direction	208 mm	219 mm	250 mm

Table 2
Result of analysis ignoring shear deformation

Method	Proposed		Orbison's
Plastic strength surface	LRFD	Orbison	Orbison
Ultimate load factor	1.997	2.066	2.059
Displacement at A in Y-direction	199 mm	208 mm	247 mm

The load–displacement results calculated by the proposed analysis compare well with those of Liew and Tang's (considering shear deformations) and Orbison's (ignoring shear deformations) results (Tables 1 and 2, and Fig. 6). The ratios of load carrying capacities (calculated from the proposed analysis) over the applied loads are 2.057 and 2.066. These values are nearly equivalent to 2.062 and 2.059 calculated by Liew and Tang and Orbison, respectively.

5.2. Single-story frame comprising lateral torsional buckling

Fig. 7 shows a single-bay single-story space frame. The stress–strain relationship is assumed to be elastic–perfectly plastic with 250 MPa (36 ksi) yield stress and a 200,000 MPa (29,000 ksi) elastic modulus. W21 × 44 section is used. The vertical and horizontal loads are applied simultaneously.

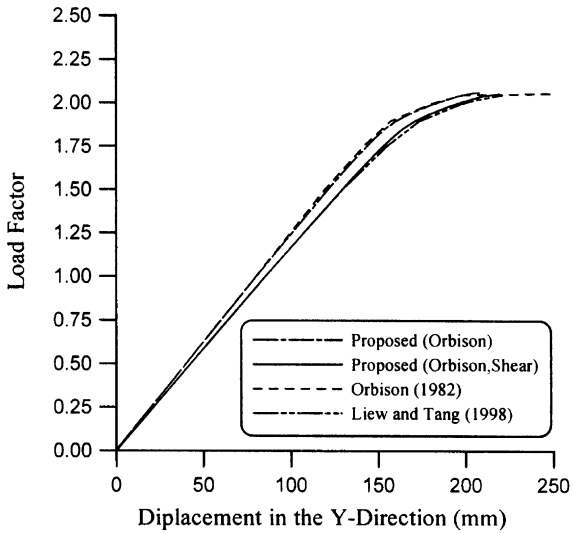

Fig. 6. Comparison of load–displacement of six-story space frame.

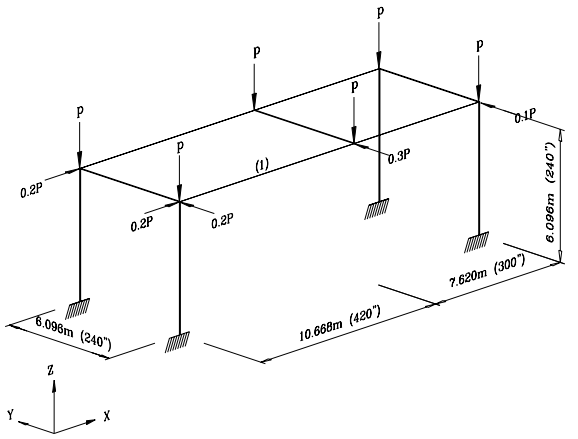

Fig. 7. 3-D, single-bay, single-story frame.

The proposed analysis is carried out. When the applied load reaches 36.88 kN (8.29 kips), element (1) fails by lateral torsional buckling. At that moment, the member forces of element (1) are $P = 23.77$ kN (5.34 kips), $M_y = 12.17$ kN m (107.7 in. k), and $M_z = 94.82$ kN m (839.2 in. k). The unit value calculated by using Eqs. (13a) and (13b) is 1.00048. Thus, it is verified the proposed analysis can capture lateral torsional buckling strength accurately.

The additional loads can be sustained until the whole structural system encounters a limit state. The frame collapses when the applied load P get to 40.21 kN (9.04 kips). Additional loads of 16.44 kN (3.70 kips) are carried by the structural system after lateral torsional buckling occurs at element (1). It is the benefit of the proposed second-order plastic-hinge analysis allowing inelastic force redistribution.

6. Case study

A three-dimensional, one-bay, two-story frame was selected for the case study. Fig. 8 shows a sidesway uninhibited frame subjected to combined lateral and vertical loads. The stress–strain relationship was

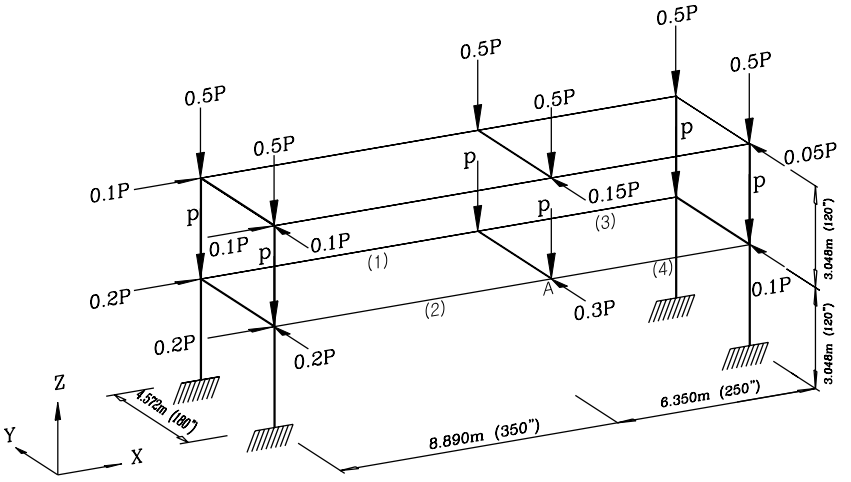

Fig. 8. 3-D, one-bay, two-story frame.

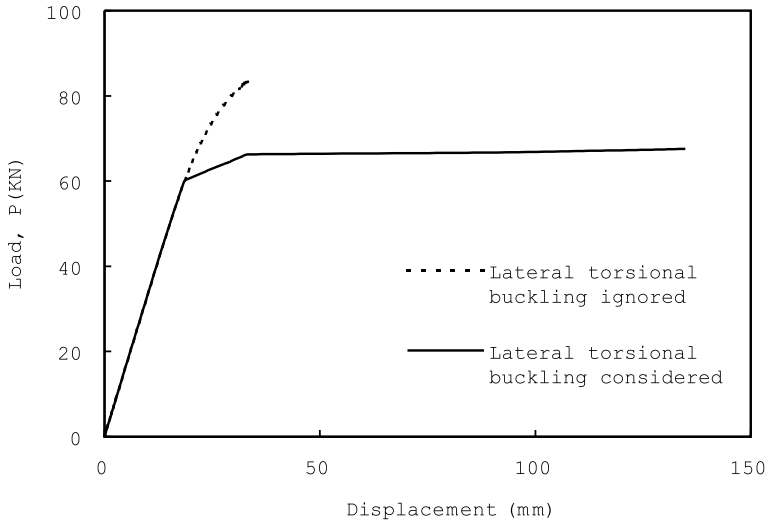

Fig. 9. Load–displacements of 3-D one-bay, two-story frame.

assumed to be elastic–perfectly plastic with a 250 Mpa (36 ksi) yield stress and a 200,000 Mpa (29,000 ksi) elastic modulus. W21 × 44 was used for all the members. Out-of-plumbness of H/500 was explicitly modeled. Two analyses are compared in this case study: the proposed and the conventional 3-D second-order plastic-hinge analysis.

In the proposed analysis, the structure collapsed by the lateral torsional buckling of elements (1)–(4b) in sequence. The load-carrying capacity P_u in term of applied load of the structural system was evaluated to be 67.57 kN (15.18 kips). If lateral torsional buckling was ignored, the frame failed by flexural buckling. The load-carrying capacity P_u of the structural system was calculated to be 83.36 kN (18.7 kips). As a result, the conventional analysis overpredict the load-carrying capacity of the frame by 1.2 times. The vertical load–displacements of the proposed and conventional analysis regarding at nodal point A are compared in Fig. 9.

The proposed analysis predicts reasonably well the degradation of flexural strength caused by lateral torsional buckling. The load-carrying capacity determined by the proposed in the case study is directly evaluated through the analysis, so separated member capacity checks encompassed by the specification equations are not required. As a result, the proposed method is time effective in design process. The proposed analysis captures the limit state strength and stability of the structural system including its individual members, while the current LRFD and ASD method evaluate the strength of the individual member only. As a result, the proposed method can capture factor of safety for the whole structure system.

7. Conclusions

Second-order plastic-hinge analysis accounting for the effect of lateral torsional buckling has been developed. The conclusions of this study are as follows:

1. The proposed method appropriately traces the inelastic nonlinear behavior including lateral torsional buckling effect.
2. The error of the proposed analysis are less than 1% when compared with the other analyses and LRFD results.

3. When lateral torsional buckling effect is ignored for the case study, the analysis overestimates the strength by more than 1.2 times. Thus, lateral torsional buckling is a very crucial element to be considered in 3-D second-order plastic-hinge analysis.
4. Compared to LRFD and ASD, the proposed method provides more information on structural behavior through a direct second-order plastic-hinge analysis of the entire system.
5. The proposed analysis can capture factor of safety for the structural system. It is more advanced than the current LRFD and ASD evaluating the strength of the individual members only.
6. The proposed analysis can be used in lieu of costly plastic-zone analysis, and it can be a powerful tool for use in daily design.

Acknowledgements

This work presented in this paper was supported by funds of National Research Laboratory Program (grant no. 2000-N-NL-01-C-162) from Ministry of Science and Technology in Korea. Author wishes to appreciate the financial support.

References

AISC, 1993. Load and Resistance Factor Design Specification for Steel Buildings. American Institute of Steel Construction, Chicago.

AISC, 1994. Load and Resistance Factor Design Specification, second ed. American Institute of Steel Construction, Chicago.

Chen, W.F., Kim, S.E., 1997. LRFD Steel Design Using Advanced Analysis. CRC Press, Boca Raton, FL.

Chen, W.F., Lui, E.M., 1992. Stability Design of Steel Frames. CRC Press, Boca Raton, FL.

Clarke, M.J., Bridge, R.Q., Hancock, G.J., Trahair, N.S., 1992. Benchmarking and verification of second-order elastic and inelastic frame analysis programs in SSRC TG 29 workshop and monograph on plastic hinge based methods for advanced analysis and design of steel frames. In: White, D.W., Chen, W.F. (Eds.), SSRC. Lehigh University, Bethlehem, PA.

CSA, 1989. Limit States Design of Steel Structures, CAN/CAS-S16.1-M89. Canadian Standards Association.

CSA, 1994. Limit States Design of Steel Structures, CAN/CAS-S16.1-M94. Canadian Standards Association.

ECCS, 1984. Ultimate limit state calculation of sway frames with rigid joints. Technical Committee 8, Structural Stability Technical Working Group 8.2. System publication No. 33, p. 20.

ECCS, 1991. Essentials of Eurocode 3 Design Manual for Steel Structures in Buildings. ECCS-Advisory Committee 5. vol. 65, p. 60.

Hechtman, R.A. et al., 1995. Lateral buckling of rolled steel I-beams. Proceedings ASCE 81 (797), 797-1–797-33.

Ilyushin, A.A., 1956. Plasticitė-Deformations Elasto-Plastiques. Eyrolles, Paris.

Kim, S.E., Chen, W.F., 1996a. Practical advanced analysis for braced steel frame design. ASCE, Journal of Structural Engineering 122 (11), 1266–1274.

Kim, S.E., Chen, W.F., 1996b. Practical advanced analysis for unbraced steel frame design. ASCE, Journal of Structural Engineering 122 (11), 1259–1265.

Kim, S.E., Park, M.H., Choi, S.H., 2001. Direct design of three-dimensional frames using practical advanced analysis. Engineering Structures 23 (11), 1491–1501.

Kitipornchai, S., Trahair, N.S., 1974. Elastic behavior of tapered monosymmetric I-beams. Research Report R239, Department of Civil Engineering, University of Sydney, Sydney, Australia.

Kitipornchai, S., Trahair, N.S., 1975. Buckling of inelastic I-beams under moment gradient. ASCE, Journal of Structural Engineering 101 (ST5), 991–1004, Proc. Paper11295.

Liew, J.Y., White, D.W., Chen, W.F., 1993. Second-order refined plastic hinge analysis of frame design: Part I and II. Journal of Structural Engineering, ASCE 113, 721–739.

Liew, J.Y., Tang, L.K., 1998. Nonlinear refined plastic hinge analysis of space frame structures. Research Report No. CE027/98, Department of Civil Engineering, National University of Singapore, Singapore.

Lui, E.M., Chen, W.F., 1986. Analysis and behavior of flexibly jointed frames. Engineering structure 8, 107–118.

Maleck, A.E., White, D.W., Chen, W.F., 1995. Practical application of advanced analysis in steel design. Proceeding the 4th Pacific Structural Steel Conference, vol. 1, Steel Structure, pp. 119–126.

Orbison, J.G., 1982. Nonlinear static analysis of three-dimensional steel frames. Report No. 82-6, Department of Structural Engineering, Cornell University, Ithaca, New York.

Prakash, V., Powell, G.H., 1993. DRAIN-3DX: Base program user guide, version 1.10. A computer program distributed by NISEE/computer applications. Department of Civil Engineering, University of California, Berkeley.

Rondal, J., Maquoi, R., 1979. Single equation for SSRS column strength curves. Journal of the structural Division, ASCE 105 (STI), 247–250.

Sawer, H.A., 1961. Post-elastic behavior of wide flange steel beams. Proceedings ASCE 87 (ST8), 43–71.

Standards Australia, 1990. AS4100-1990, Steel Structures, Sydney, Australia.

Vogel, U., 1985. Calibrating frames. Stahlbau 10, 1–7.

White, D.W., 1960. Inelastic lateral instability of beams and their bracing requirements. Ph.D. Thesis, Lehigh University, Bethlehem, PA.

White, D.W., 1985. Material and geometric nonlinear analysis of local planar behavior in steel frames using iterative computer graphics. M.S. Thesis, Cornell University, Ithaca, NY, p. 281.

Ziemian, R.D., McGuire, W., Dierlein, G.G., 1992. Inelastic limit states design. Part II: three-dimensional frame study. ASCE Structure Engineering 118 (9), 2550–2568.